

Chapter 2

Cadmium-Based Nanomaterials

Nanotechnology is unquestionably a greatest discovery of current human generation. It is a complicated science involving unique strategies, synthesis procedures, characterization techniques, and applications of materials at scale of one billionth of a meter. At this very scale, quantum physics comes into action to explain the behavior of materials where the individual atoms, molecules and their interconnecting assemblies possess novel phenomenon due to quantum confinement and energetics. Moreover, the increased surface-to-volume ratio associated with this business causes an enhancement of interactions with the external world. These considerations and exciting properties related to nanomaterials have led the scientific world to an engrossment which has resulted into the current progress in the fields of nanostructures, their fabrication, and implementation.

2.1 Introduction to the Nanotechnology and Nanomaterials

The technological development and the related glamor have fascinated the experts as well as beginners towards the cosmos of this novel class of materials. These materials with astonishing structural, optical, and electronics properties provide great evolution in applications related to different fields of life at domestic as well as industrial levels. Nanomaterials are the starting stone of nanotechnology having at least one dimension within scale of 100 nm. This length scale has provided a driving force to renovate the existing technology with unprecedented technological benefits in applications related to information, communication, energy, optoelectronics, photovoltaics and facilities related to daily life. The structure of materials at this scale allows the control of important properties without shifting the basic chemical properties. These materials are important due to their entirely exceptional physical properties based on their unique structure, shape, and morphological features. The downscaling of bulk materials to the nanoregime causes changes in energetics involving electronic energy

levels. The packing of elementary atomic or molecular species to produce nanomaterials produces almost an infinite number of structural arrangements of molecules leading to abundant possibilities of lattices and energy levels. These energy levels introduce principal bands separated by band gap which is a key finger print of the electronic materials. The materials are normally considered as semiconductors when they exhibit band gaps up to about 3.8 eV. The electronic properties based on density of states, energy levels diagram, and band structure are significantly altered when an electronic material is thinned down to nanoscale. The energy levels are very close and hence they can be described as continuum to produce conduction and valance bands whose gap is usually higher for nanomaterials as compared to the bulk counterparts. The transfer from indirect to direct band gap has also been observed when bulk materials are converted to nanoscale. It points to engineering of electronic properties which opens up a large number of opportunities for the material scientists to utilize such materials for ongoing and future applications.

In recent years, this engineered technology has led the workers to tailor the properties of conventional materials into desired functionalities by realizing novel nanomaterials having extraordinary properties. For example, carbon atoms are structured in a bit loose interlayer pattern to produce graphite used in refractories, batteries, and pencils. The strong bonding of these carbon atoms in three-dimensional covalent network throughout the lattice produces very hard structure of diamond. Another allotropic form of carbon is known as graphene in which carbon atoms are bonded in two-dimensional sheet-like structures to produce hardest ever-known material. The graphene is a monolayered nanomaterial which has exhibited exceptional properties for variety of applications. Carbon nanotube is another allotropic form of carbon which has presented largest length-to-diameter ratio and offers excellent thermal, electrical, and optical properties. Fullerene in the form of buckyballs is another allotropic form of carbon in the form of nanomaterial. Several other examples may be quoted which shed light on provision of new properties upon structural evolution as well as thinning of bulk materials to their nanoscale counterparts. For example, nanocrystalline form of copper is harder as compared to the micro-sized crystalline copper.

The nanostructured materials are obtained in form of thin films, clusters, multilayers, and in the form of nanocrystalline structures having 0, 1, 2, and 3 dimensions. These materials may categorize in the form of metals, alloys, compounds, semiconductors, etc., in various crystal structures, shapes, and morphologies. Following sections shed some light on relevant features of nanomaterials.

2.2 Structure of Nanomaterials

Crystal structure and crystallography are key features of nanomaterials which put direct influence on their properties. The crystallinity directly affects the surface chemistry as well as physical properties of the nanomaterials. The crystal structure can be changed as per elemental composition, elemental ratio, and packing geometry

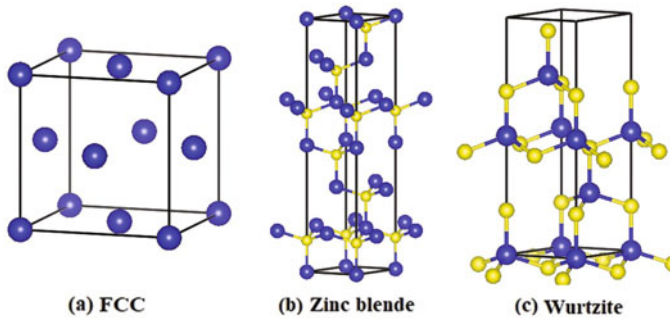


Fig. 2.1 Illustration of typical crystal structures, **a** face centered cubic, **b** cubic zinc blende and **c** hexagonal wurtzite

and nature of bonding of constituents (Guo and Tan 2009). The nanomaterials of cadmium containing II–VI semiconducting materials are usually crystallized into face-centered cubic (FCC), cubic zinc blende (ZB) and hexagonal wurtzite (WZ) crystal structures (Fig. 2.1).

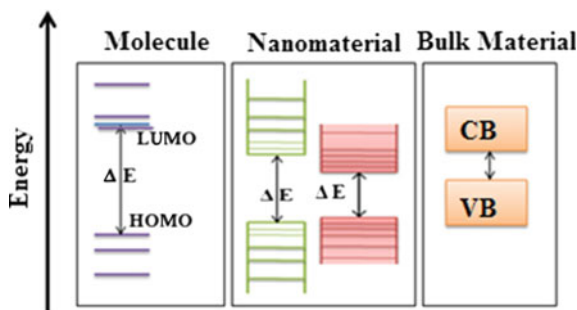
2.3 Properties of Nanomaterials

The robustness of nanostructures is simply due to their exceptional properties which appear upon downscaling the materials from bulk to their nanoscale. The extraordinary response of nanostructured materials depends basically upon the following two features (Mews et al. 1994).

1. The quantum size effect: The electronic structure of the materials is strongly size dependent.
2. The surface/interface effect: The surface-to-volume ratio of nanomaterials is significantly higher.

The physical qualities of the nanomaterials are mostly explained by considering the quantum size effect and the investigation of this effect has become a primary criterion to characterize the materials. Due to the diverse degrees of confinement of particles (with different dimensions), the band gap energies of the nanostructure changes significantly (Yu et al. 2003a, b). Correspondingly, the size and dimensionality determines electronic and electrical properties of the materials. In nanostructured materials, the band edge states are closely packed because of the dimensionality and quantization. It points to tailoring the band diagram of nanomaterials and availability of diverse optical transitions. The II–VI semiconducting nanomaterials exhibits unique optical properties, particularly the semiconductors which have direct band gaps (Djurišić and Leung 2006; Arora and Sundar 2007). The particles scattering at the boundaries of the nanostructures have an effect on the

Fig. 2.2 Evolution of band diagram of bulk material from molecular structures to exhibit a link to nanomaterials



electronic properties, showing an increase in resistivity because of large surface scattering. In nanomaterials, the energy of surface atoms plays very significant role in determining their characteristics (Aqra and Ayyad 2014). An illustration showing the comparison of energy levels and band gaps of nanomaterials with the bulk material and molecular structures is given in Fig. 2.2.

The enhanced surface-to-volume ratio sheds light onto the surface free energy and availability of abundant place in nanomaterials to interact with the external world. For nanostructured materials, the surface energy is higher than bulk atoms which causes enhancement in chemical reactivity of nanosized materials (Li et al. 2015). On the same lines, the biological cells operate in a different way with the nanomaterials than bulk (Wong et al. 2013). The interface effect is also an important function to describe the chemical properties which are of prime importance in case of catalysis. This effect has got prime importance to explain exceptional characteristics of nanomaterials; e.g., specific heat, thermal conductivity, optical response, etc. In comparison with the bulk, the nanomaterials usually have low melting points, reduced lattice constants, higher band gaps, varied thermal stability, and enhanced surface interactions (Cao 2004).

2.4 Morphology of Nanomaterials

One important aspect of nanomaterials is surface morphology which is highly dependent upon synthesis strategies and leaves strong impact on properties of the materials for utilization in different applications. To investigate the morphology of NCs is of prime importance just after synthesis of the nanomaterials since it gives information about size, shape, structural arrangement, and surface of species of the obtained material. The nanomaterials have properties different from their bulk counterparts. The dimensional features of a solid play important role to determine its properties and it has been established that upon sufficient reduction in the dimensions the characteristics of the materials become remarkably different from those of the starting bulk solid. As the size of the solid material is reduced, the considerable modifications in the optical, electrical, chemical, and magnetic properties can be

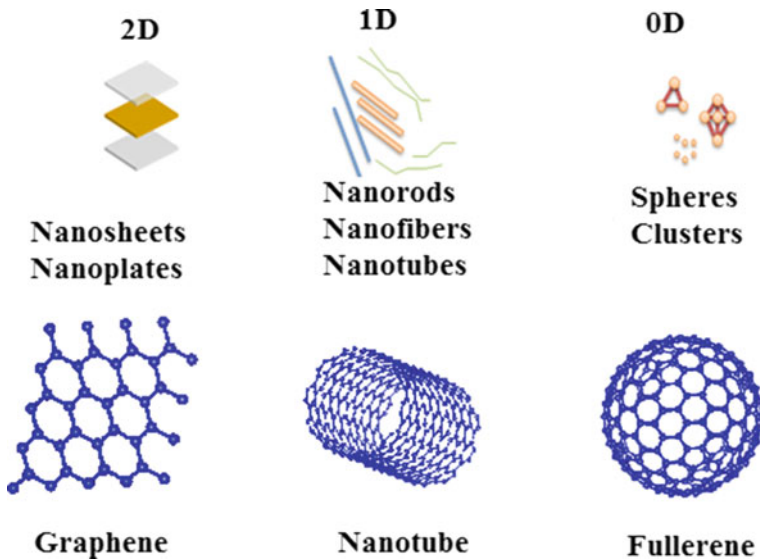


Fig. 2.3 Types of nanomaterials based on size, shape, morphology, and dimensionality of structural units. The examples from carbon allotropes are also given

introduced. The electrons and holes confined in a low-dimensional system behave significantly different and leave strong impact on performance of the devices based on such quantum size effects. The materials are classified according to the format given by Pokropivny and Skorokhod (2007) into several categories; (i) Three-dimensional (3D) structures (nanocups), (ii) Two-dimensional (2D) structures including nanofilms, nanosheets, nanolayers nanoslabs, etc. (iii) One-dimensional (1D) structures like NWs, nanorods(NRs), nanobelts (NBs), etc. (iv) Zero-dimensional (0D) structures as NPs, nanospheres, nanodots, etc. (Fig. 2.3).

2.4.1 Three-Dimensional (3D) Structure

In such materials, the particle motion is not quantized in any direction and they can freely move in the material. These materials have large surface area and offer several distinctive properties on the basis of enhanced surface-to-volume ratio and quantum confinement effects (Khalily et al. 2016). There is a great research attention in realization of these materials for several applications (Hu et al. 2009). 3D nanocups as Second Harmonic Generators (SHG) have been used for generation of second harmonic light with rising strength (Zhang et al. 2011). SHG gives a capability to devise and manufacture well-established second-order nonlinear nanomaterials. The performance of 3D nanomaterials can be increased by controlling the structure, size, and morphology in its broad range of applications as

Table 2.1 The classification of nanomaterials and their sizes on the basis of dimensionality

| Nanostructures | Characteristic nanoscale dimensions |
|---------------------------------------|-------------------------------------|
| 2D structures (nanosheets, nanoslabs) | 1–1000 nm (thickness) |
| 1D structures (NWs, NTs) | 1–100 nm (radius) |
| 0D structures (QDs) | 1–10 nm (radius) |
| Porous material | 1–50 nm (pore size) |

batteries (Kamarudin et al. 2009), electrodes (Kargar et al. 2013) and catalysis (Sun et al. 2011; Shi et al. 2016).

Unlike for the case of bulk solids, there are several novel physicochemical characteristics which can be exploited for applications by suitable control of size, shape, morphology, and structural arrangement in case of nanomaterials. The conversion from a three-dimensional material to a low-dimensional nanostructure usually enhances the band gap value of that material (Moras et al. 1996). The number of reductions in dimensions frequently categorizes the different low-dimensional nanostructures. The number of degrees of freedom in case of particle momentum is controlled by the dimensionality of the material. The classification of nanostructures on the basis of dimensionality and granular size is given in Table 2.1.

2.4.2 Two-Dimensional (2D) Structure

Thin films, nanoplates, nanosheets, nanodisks, and nanoslabs are few examples of the two-dimensional nanomaterials (Fox 2002). Recently, 2D nanomaterials have attained great attention in research due to exceptional reactivity and shape-dependent properties and consequent use in nanotechnology (Buhro and Colvin 2003). Graphene is a well-known 2D nanomaterial having atomic thickness and its every atom is available to react with the external world. These materials are very attractive for understanding the nanostructure synthesis as well as for exploring advanced applications in many fields like sensors, electrocatalysis (Yu et al. 2015), and photocatalysis etc. (Luo et al. 2016).

Nanosheets of alloyed CdS and ZnS have been prepared with different Cd and Zn concentrations and it was observed that $\text{Zn}_{0.7}\text{Cd}_{0.3}\text{S}$ and $\text{Zn}_{0.88}\text{Cd}_{0.12}\text{S}$ nanosheets showed higher emission intensity (Fig. 2.4b). Exclusive MoS_2/CdS heterostructure showed striking properties used in solar energy conversion process with quantum yield of 41.37% at 420 nm and hydrogen evolution reaction $49.80 \text{ mmol g}^{-1} \text{ h}^{-1}$. These MoS_2/CdS nanosheets on nanorod revealed their applications for inexpensive photocatalysts for water splitting (Yin et al. 2016). CdS NPs decorated Cd nanosheets (CdS NP/Cd NSs) confirmed a notable improvement in visible-light activated photocatalytic performance for hydrogen production (Shang et al. 2016).

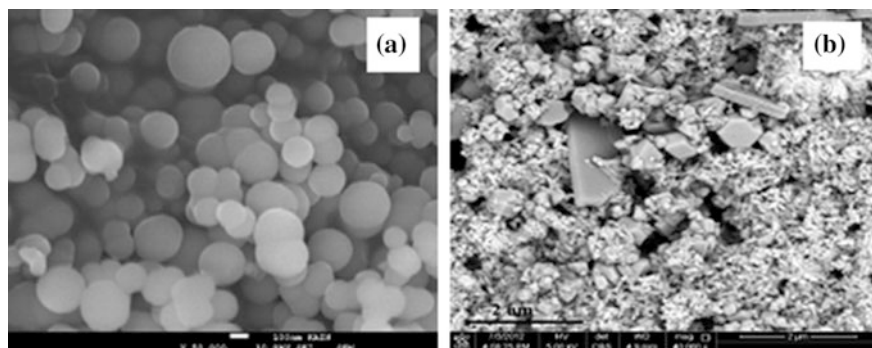


Fig. 2.4 **a** SEM image of CdO NPs with size ranging from 40 to 100 nm (Aldwayyan et al. 2013). © Open access **b** FESEM image of $\text{Zn}_{0.88}\text{Cd}_{0.12}\text{S}$ nanosheets (Mahdi et al. 2013). © Open access

2.4.3 One-Dimensional (1D) Structure

In 1D material, the motion of electrons and holes is confined in two directions. These materials have diverse optical and electronic properties because of their 2D confinement. NWs, nanofibers, NTs, NBs, quantum wires, NRs, nanoribbons and nanospindles are renowned 1D structures which have been synthesized.

NTs is an interesting class of 1D nanomaterials. Metal NTs showed more exciting catalytic properties than that of their respective NPs (Tang et al. 2013; Ge et al. 2016). Due to special surface plasmon effect, NBs can be adjusted in order to absorb or emit light in particular direction. As the gas atoms are adsorbed on the surface, they act like flow of current which allows the utilization of the respective material as analogous to FETs. NBs have properties analogous to the NWs; displaying FET-like performance and functional surface. NBs have desirable and exclusive qualities due to their surface area which makes them attractive for applications in nerve gas sensors, ethanol detectors, and hydrogen gas sensors. These structures have also been considered as suitable candidates to fabricate novel optoelectronic devices, like in LEDs, laser diodes, detectors, and optical sensors (Huang et al. 2015). NRs are promising materials for use as multifunctional material due to its high sensitivity, uniform morphology, and light detection ability. These nanomaterials can be created using different materials like metals, metal oxides, and organic materials. The size-dependent properties of NRs were studied in range 1–10 nm. ZnO/CdS and ZnO/CdO NRs showed great potential for use in gas sensing mechanism (Kim et al. 2016). A list of some famous nanomaterials having different morphologies with their properties and applications is shown in Table 2.2.

Owing to the ability to confine the electromagnetic waves into one particular direction, 1D nanomaterials are found potential candidates to function as waveguides. 1D nanomaterials offer important features for technological applications due to their extraordinary optical, magnetic, electrical, and chemical characteristics

Table 2.2 Some famous nanomaterial types, their morphology, synthesis strategies and applications

| Types of nanostructures | Typical size | Mostly used synthesis methods | Properties | Applications |
|-------------------------|--|---|--|---|
| QDs | 2–3 nm and 5–6 nm | Solvothermal, hydrothermal, aqueous synthesis | Tunable absorption spectrum, high extinction coefficient, high quantum yield, water splitting, hydrogen production | Quantum computation, solar cells, LEDs, biology, photocatalysis, photodetectors |
| Clusters | Less than 2 nm | Pulsed laser deposition, wet chemical methods, arc discharge method, ion sputtering | Large surface-to-volume ratio | Catalysis, solar cells, fluorescence bio-imaging, bio-labeling, detectors, photoluminescence, biosensor |
| NRs | 1–100 nm Standard aspect (l/w) ratio 3–5 | All wet chemical synthesis methods, condensation evaporation, pulsed laser deposition | linearly polarized emission, large absorption cross-sections, amplifying stimulated emission and lasing | Displays, cancer therapeutics, LEDs, sensor, photovoltaic |
| NWs | 10 ⁻⁹ m l/w ratio is 1000 | CBD, SILAR, electrodeposition, polyol synthesis | Uniform morphology, huge surface area, high conductivity, high chemical reactivity | Thermoelectric cooling system, energy conversion devices, junction diode, memory cells and switches, lasers |
| NTs | Less than 100 nm diameter, and ½ nm thick wall | CVD, CBD, microemulsion, microwave synthesis, polyol synthesis | High length-to-diameter ratio | Energy storage, fuel emission, biomedical applications |
| Nanosheets | 1–100 nm thick (graphene nanosheet 0.34 nm thin) | Co-precipitation, hydrothermal, solvothermal | Crystalline surface, anisotropic confinement of nanospaces, layered thinness, colloidal properties | Photovoltaic, meta-materials, chem/biosensors, photochemistry |

(Tang et al. 2002; Zhao et al. 2008; Qi et al. 2012). Until now, numerous synthesis methods have been employed to prepare the 1D nanostructures like electrochemical synthesis (Wu et al. 2010), microwave-assisted synthesis (Liu et al. 2010; Lu et al. 2004), inert gas condensation, spark discharge method, spray pyrolysis, thermal plasma, solvothermal (Ghoshal et al. 2009), sono-chemical, template method (Cao

and Liu 2008), and polyol process (Mayers and Xia 2002a, b; Ma et al. 2011; Yang et al. 2010; Zhu et al. 2011). Despite establishment of a number of these and other methods, achieving an easy, straightforward, inexpensive, and convenient method to provide high yield of 1D nanomaterial is still a challenge.

2.4.4 Zero-Dimensional (0D) Structure

The reduction of the size of bulk material near the value of its Bohr radius gives us the system with zero dimensions (Alivisatos 1996). These materials belong to an extraordinary class of semiconducting materials and offer quantization in three directions. Their quantized energy levels relate them more strongly to the molecules rather than the bulk materials.

QDs (QDs), spheres, and clusters are examples of 0D materials in which the motion of particle is fully confined. QDs are small crystals of semiconducting materials with radius of 1–5 nm and exhibit exclusive electronic characteristics in-between bulk and molecules. QDs are also known as “fluorescent NPs” and can exhibit any color of light by simply altering their size (Hu et al. 2011). Their emission color can also be varied by changing their composition through doping process. They can be categorized as core, core/shell, and alloyed QDs. Core-type QDs are single constituent materials with homogeneous compositions like CdS, CdSe, ZnS, etc. Core/shell QDs have small section of one material enclosed in a different material like CdSe in core and ZnS is shell (Wei et al. 2015). The knowledge of the physical and chemical characteristics of the core/shell QDs provides information on their use in light emission technology. Pan et al. synthesized the CdSe/CdS QDs at 180/140 °C in an autoclave with core size varying between 1.2 and 1.5 nm. These nanostructures showed dominant peaks in emission spectra ranging from 445 to 517 nm with quantum yield (QY) of 60–90%. Spherical CdO NPs with uniform size of 50 nm and some particles have joined with size of 100 nm were obtained, as shown in Fig. 2.4a.

Alloyed QDs structured obtained after alloying two semiconductors with dissimilar band gap values have revealed unique and fascinating characteristics. The alloyed QDs have not exhibited only quantum confinement effect but also presented composition-tunable characteristics. Highly emissive alloyed $\text{CdSe}_x\text{S}_{1-x}$ QDs showed the photoluminescence (PL) peak at 490 nm with absolute QY of 79% (Zhang et al. 2016). At present, QDs are utilized for numerous biological, biomedical (Plaza et al. 2016), optical and optoelectronic applications, varying from biosensors to solar cells (He and Ma 2014). The electronic properties of these materials are directly linked to the size and shape of the nanostructures.

A variety of techniques is available to prepare the 0D nanomaterials, like mechanochemical ball milling, ion sputtering, molecular beam epitaxy (MBE), inert gas condensation, pulsed laser ablation, sono-chemical, electrodeposition, microwave-assisted, sol-gel, solvothermal, CVD and laser pyrolysis etc. Each

method has its own benefits. Thermal plasma is also used for preparation of 0D materials due to its high reactivity, high enthalpy, rapid quenching and also exceptional characteristic of plasma to provide proficient solution.

2.5 Cadmium Chalcogenide Nanomaterials

The nanomaterials comprising of compounds of elements II and VI groups of periodic table are termed as II–VI semiconducting nanomaterials. At absolute zero temperature, they behave like the insulator but at finite temperature they present temperature-dependent properties of conductors and insulators. In case of these compounds, if cation is cadmium (Cd) and anions is taken from list of chalcogens (oxygen, sulfur, selenium, tellurium) in group 16 of periodic table, the resulting group of materials (CdO, CdS, CdSe, CdTe) will be referred as cadmium chalcogenides. Generally, these materials are synthesized as zinc blende (cubic) structure (Majid et al. 2015; Ranjithkumar et al. 2016) and represent the semiconducting properties. There is inversion symmetry present in these materials and some important bulk parameters of cadmium chalcogenides are shown in Table 2.3. The materials with such properties can be used for optoelectronic and piezoelectric applications (Willardson and Beer 1977). At present, the II–VI semiconductor materials have fascinated many investigators for their remarkable physical properties which are due to their three-dimensional confinement of carriers and increase in the number of surface atoms (Zhang et al. 2007). These semiconductors in analogous nanocrystalline form have become center of attention because of their tunable band structure (Kamat 2008), high extinction coefficient (Yu et al. 2003a, b) and possible multiple exciton generation (Nozik 2002). These materials have shown unparalleled potential to cover the extensive range of expositions in optoelectronic devices and photovoltaics (Zhu et al. 2015; Xu et al. 2014).

This class of II–VI semiconductors materials has got prime research and industrial attention because of their innovative characteristics along with size- and shape dependence of these properties. The nanomaterials display functional characteristics not available in their bulk correspondents. A subclass of these nanomaterials with size of 2 nm or less exhibit some additional properties to be utilized in advanced technology (Harrell et al. 2013). The synthesis strategies and characterization of the materials CdO, CdS, CdSe, and CdTe in nanoscale, whose cationic and anionic

Table 2.3 Important parameters of bulk CdO, CdS, CdSe, and CdTe semiconducting materials at 300 K (Jefferson et al. 2008; Thirsk 1989)

| Nanomaterial | Structure | E_{gap} (eV) | Lattice parameters (Å) | Density (kgm^{-3}) |
|--------------|-------------|-----------------------|------------------------|-------------------------------|
| CdO | FCC | 2.16 | 4.69 | 8150 |
| CdS | Wurtzite | 2.49 | 4.13/6.71 | 4820 |
| CdSe | Wurtzite | 1.74 | 4.3/7.01 | 5810 |
| CdTe | Zinc blende | 1.43 | 6.48 | 5870 |

Fig. 2.5 Part of periodic table showing the cationic and anionic components of cadmium containing II–VI semiconducting materials described in this book

| | II | III | IV | V | VI |
|---|----------|----------|----------|----------|----------|
| 2 | | 5 B | 6 C | 7 N | 8 O |
| 3 | | 13 Al | 14 Si | 15 Zn | 16 S |
| 4 | 30 Zn | 31 Ga | 32 Ge | 33 As | 34 Se |
| 5 | 48 Cd | 49 In | 50 Sn | 51 Sb | 52 Te |

composition are shown Fig. 2.5 is primary theme of this book. The QDs based on these materials revealed extraordinary size-dependent optical characteristics with narrow band-gap. These materials have shown exceptional potential for device grade applications due to their size-tunable electronic and optical properties (Murugadoss et al. 2015; Salem et al. 2017; Zhu et al. 2013; Wageh et al. 2011).

The remaining sections of this chapter are dedicated to describe the structural, thermal, mechanical, vibrational, electronic, optical, and transport characteristics of these materials.

2.6 Properties and Applications of Cadmium Chalcogenide Nanomaterials

The cadmium chalcogenides (CdO, CdS, CdSe, CdTe) have been extensively investigated both in bulk and nanoscale. However, there is a huge interest in nanostructures of these materials due to their potential in existing and future applications. These materials are recognized with great promise for photovoltaics due to their high light sensitivity and quantum efficiency. Furthermore, the range of their direct band gap indicates the opportunity to manufacture optoelectronic devices with response to different electromagnetic radiations. However, the flexibility of these devices is restricted by the dissimilar band gap for individual material. The structural arrangement of their heterostructures can make these semiconductors to present good performance since they offer “band engineering” opportunities. Currently, utilizing the QDs for solar energy yield has become a striking field for research. In such systems, the photoexcited electrons are transferred to the large band gap of TiO₂ and ZnO semiconductors. In contrast with other sensitizers the semiconductor QDs exhibit superior properties due to their sizes.

Their band gap can be varied by changing the size of QDs and they can form many excited charged particles with the impulse of a single photon (Gao et al. 2009; Nozik 2002). Nanoscale hetero-, core/shell, and hierarchical structures are formed by combining the two materials with same chemistry-, size-, and material-dependent properties show more efficiency and multifunctionality than their single structures. CdTe-sensitized TiO_2 NTs have been synthesized and studied with enhanced photo-electro-chemical activity (Gao et al. 2009). A summary of these materials with their applications is given in Fig. 2.9.

2.6.1 Cadmium Oxide

Cadmium oxide (CdO) exhibits distinctive properties when compared to other cadmium chalcogenides. Translucent conductive oxides (TCOs) have been studied with superb photoelectronic behavior because of low specific resistance and high transmittance. Among all TCOs, the study of CdO nanomaterials is highly attractive and exciting field. CdO is a binary compound of cadmium and oxygen which is normally obtained in NaCl-like cubic structure (Brock 2004). It is n-type semiconductor, insoluble in water and soluble in mineral acids. It has direct and indirect band gap with values of energy as 2.28 and 0.55 eV respectively. There is a worthwhile research consideration for CdO because of its fascinating features such as its low electrical resistivity and concurrently high transparency in the visible region (Afify et al. 2014).

CdO nanomaterials synthesized with different morphologies show excellent properties. Cadmium interstitials are shallow donors and oxygen vacancies produce deep levels in band gap of CdO NPs, therefore their study is worthwhile to explore the luminescence process (Goswami and Choudhury 2015). High density and ordered CdO NW array with diameter ~ 50 nm and length ~ 2.5 μm showed high transmittance over 80% in visible region (Chaure 2016). These homogeneous and vertically aligned NW arrays exhibited direct band conversion at 440 nm and exciton emission at 510 nm.

In the biomedical field, CdO nanopowders play a vital role due to their antibacterial properties. These microstructures proved their significant antibacterial and antifungal capabilities against pathogenic bacteria and fungi strains because of (i) formation of reactive oxygen species (ii) discharge of Cd^{2+} ions (iii) the size and morphology of the product nanopowders (Balamurugan et al. 2016). CdO nanopowders can be applied as efficient antimicrobial agent against the pathogenic microorganisms. Unique rhombus-like structure of CdO showed the photocatalytic performance for the degradation of different pollutants like CR, MG, and CV (Tadjarodi et al. 2014).

Recently, highly capable flower-like CdO-SiO₂ nanomaterial was prepared and studied. It has shown good photodegradation performance under UV light irradiation for Rhodamine B dye and maximum degradation was observed at pH value 7 (Senthilvelan 2017). The current–voltage characteristics of CdO/Si devices have been studied in light and darkness which revealed high sensitive reactivity in the

visible and the near IR regions of electromagnetic spectrum (Ortega et al. 2000). A needle-shaped CdO NC shown in Fig. 2.6b, exhibited single crystalline and uniform structure. These nanostructures showed excellent response to infrared light and diluted NO₂ gas, and they have ability to absorb IR light due to their indirect band gap. This indicated the potential of the material to be applied as infrared photo-sensors and poisonous gas detectors. Due to high surface area, CdO NTs (Fig. 2.6a) showed potential to be applicable in fields of nanooptics, catalysis, and nanosensors. NBs of CdO mostly have length below the 100 μm scales and characteristic width ranging between 100 and 500 nm.

Like bulk materials, the process of doping also greatly affects the properties of nanomaterials. The nanostructures of CdO doped with different metals have been studied, e.g., including light metals Li (Dakhel 2011b), B (Yakuphanoglu 2011), transition metals like Ti (Gupta et al. 2008), Zn (Dakhel 2012) and some rare earth metals like Gd (Alemi et al. 2013), Ce (Dakhel 2011a). Doping of Cu in CdO improved its optical transmittance in visible range. The prepared NWs showed good activity to be applied in optoelectronic devices (Benhaliliba et al. 2012). CdO nanofilms showed an increase in band gap energy after doping with Bi, due to quantum size effect (Dagdelen et al. 2012). The current–voltage results and other electrical measurements showed CdO nanofilms acts as electron transport layer (Soylu and Kader 2016). These nanofilms layered on *p*-Si (a photodetector) CdO/*p*-Si heterojunction revealed the properties of a rectifier diode and a well-built photoreactive response.

An appropriate thermal treatment and accordingly the variations in morphology and electrical behavior of CdO based nanostructures have exposed a wire-to-rod conversion and reduction of electrical resistance (Krishnakumar et al. 2011). These CdO nanofilms proved to be appropriate candidate as CO₂ sensors for useful applications. Highly crystalline CdO nanostructures have been studied as detecting layer in resistive detectors and exhibited high reactivity to NO₂ at low working temperature of 100 $^{\circ}\text{C}$ and high selectivity against CO (Rajesh et al. 2014).

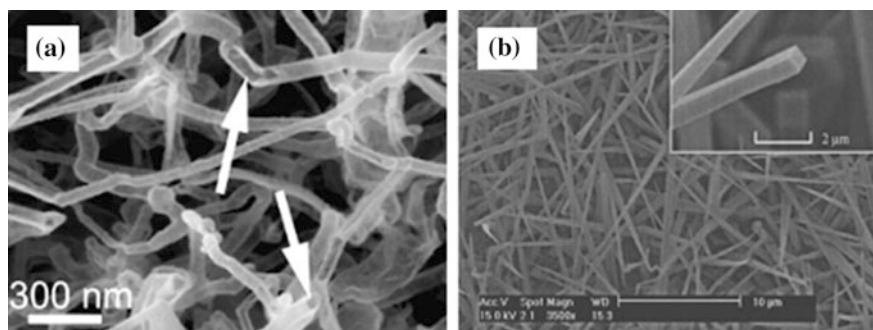


Fig. 2.6 **a** SEM image of thermally synthesized CdO NTs. White arrows indicate the hatches of NTs (Lu et al. 2008). © 2008 Elsevier **b** SEM image CdO nanoneedles with a square cross section (Liu et al. 2003). © 2003 American Institute of Physics

The exclusive properties of CdO makes it a potential candidate for photodiodes (Soylu and Kader 2016), phototransistors, photovoltaic cells (Usharani et al. 2015), transparent electrodes (Tang et al. 2015), solar cells (Radi et al. 2006), liquid crystal displays (Baranov et al. 1997), photodetectors (Ortega et al. 2000), gas sensors (Rajesh et al. 2014) and spintronics etc. (Thovhogi et al. 2016; Thema et al. 2015; Jimenez-Perez et al. 2015). It has attraction for use as a gas sensing material due to its liquid petroleum gas sensing properties (Waghulade et al. 2007). Such extraordinary properties and multifunctionality of CdO has given it a valuable place in the family of nanomaterials.

2.6.2 Cadmium Sulfide

Cadmium sulfide (CdS) is a binary compound of cadmium and sulfur. Its bulk structure has a hexagonal wurtzite structure with melting point 1600 °C (Goldstein et al. 1992) and is insoluble in water, but soluble in dilute mineral acids. It is an n-type semiconductor. It has a deep acceptor level and shows conductivity due to sulfur vacancies. At room temperature, the bulk structure of CdS has the value of band gap energy 2.42 eV, (Rajeshwar et al. 2001) and this value of energy shows that it is one of the most capable applicant for sensing visible light (Singh and Chauhan 2009). With the modifications in reaction conditions, CdS shows the corresponding changes in its 1D morphology. Band gap of CdS straightforwardly can be tuned through preparing the ternary alloys with CdSe to be applied in tunable photodetectors (Takahashi et al. 2012). Though CdS has a number of applications in bulk form but its conversion into nanoscale provide exceptional physical, chemical, electrical, optical, and transport properties. Due to size-dependent characteristics of the II–VI semiconductor nanostructures, 2.5 nm CdS reveal its very low melting point as ~400 °C (Goldstein et al. 1992). A change in the band gap was observed for CdS nanocrystallites with its band gap energy 3.85 eV (Banerjee et al. 2000). At high pressure a difference in its phase from hexagonal wurtzite type to rock salt cubic phase was also observed (Chen et al. 1997).

Different structures of CdS shows different properties, wurtzite CdS nanostructures have been prepared with complex morphologies (Yao et al. 2006). CdS NRs (shaped as very structured hierarchical nanoflowers), NWs (branched), and nanotrees (construct via branched nanopines) showed good photocatalytic properties. Their photocatalytic performance for the degradation of acid fuchsine has been studied and branched NWs proved to be good photocatalyst. Nanostructures of CdS can easily be tuned for emitting the visible light through variations in the initial ratios of Cd and S (Lopes et al. 2014). NBs are chemically pure and structurally homogeneous and create a class of nanostructures with 30–300 nm width, 10–30 thickness and length in millimeters (Fig. 2.7). Dielectric properties of CdS NPs have been investigated in frequency range between 50 Hz and 5 MHz (Suresh 2013). There was an increase in these properties observed at low-frequency range at diverse temperatures.

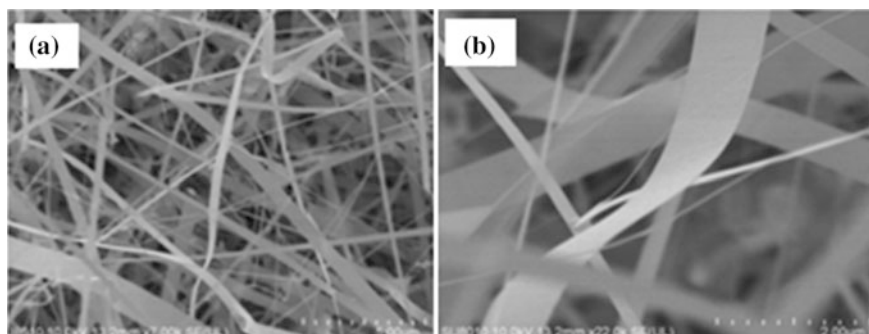


Fig. 2.7 SEM images of synthesized CdS NBs (Li et al. 2014). © Open access

At present, nanostructured mosquito larvicides have an important role for controlling the malaria vectors *Anopheles stephensi* and *A. sudaicus* (Sujitha et al. 2017). CdS NPs have been proved to be very toxic for young instars of the malaria vectors populations and also against the chloroquine-resistant (CQ-r) plasmodium falciparum parasites. This nanoproduct showed considerable affects on the enzymatic activity of non-target aquatic organisms, with unique reference to mud crabs. CdS is one of the most proficient nanomaterial for solar cells (El-Baz et al. 2016) and there are numerous applications of this material in the field of optoelectronics, photonics, photovoltaic, and photocatalysis (Rathinamala et al. 2014). CdS is also used as a pigment in paints and in engineered plastic for good thermal stability (Acharya 2009). In photonics, CdS is employed to make NCs (Dai et al. 2010). A little modification in size and morphology of CdS NPs leads to its increased photocatalytic activity (Khan et al. 2016). High-sensitivity photodetector material have been observed from CdS NTs and NWs, proving their potential as photodetectors in technological applications with high capability at low-cost (An and Meng 2016). Due to high value of surface to volume ratio, CdS nanomaterials can be used to design photocells (Samarasekara and Madushan 2016), light-emitting diodes (LEDs) (Lin et al. 2002; Murai et al. 2005), lasers (Duan et al. 2003), address decoders (Zhong et al. 2003), sensors (Travas-Sajdic et al. 2006), optical biosensors (Lin et al. 2013), optical switches (Li et al. 2010), hydrogen production (Zyoud et al. 2010), and water purification (Zhu et al. 2009). All of these striking properties points to potentials of CdS nanomaterials for ongoing and future applications.

2.6.3 Cadmium Selenide

Cadmium selenide (CdSe) is a binary compound of cadmium and selenium which shows n-type conductivity and has a band gap of 1.74 eV at room temperature. The molecular mass of CdSe is 191.37 g/mol, and appears as a dark red material (Amiri et al. 2013), it can have structures of hexagonal as well as cubic. In research, CdSe

nanomaterials have been one of the most attractive semiconducting materials unlike bulk counterparts of other members of cadmium chalcogenides. Due to their unique characteristics and applications, CdSe nanomaterials are of great interest in different fields of science and technology. The electrical and optical properties of the CdSe nanomaterials are size-dependent. These nanomaterials are extensively studied because of their adjustable band gap and reducing their size plays an important role in devices covering the whole spectrum of visible light (Qu and Peng 2002).

The coating of hydrophilic polymers enables them to be soluble in water, protect the photophysical properties of CdSe core, and secure the relatively compact dimensions (Fig. 2.8a). The shell additionally offers the surface trap states, increasing the fluorescence QY and making the nanostructures to be applied in fields of biological labeling and light-emitting devices. CdSe NPs prepared by Kalhori et al., showed the increased photoconductivity as compared to the preceding research work and photosensitivity of 110, which is also better than the earlier work (Kalhori et al. 2015). In the Fig. 2.8b, different-sized ZnS-capped CdSe QDs are shown; every test tube emits a light of diverse color, displaying the variation in size of the particles.

CdSe and CdSe/CdS NPs have been prepared by Suganthi et al. and their optical properties were studied. TEM and HR-TEM images revealed a narrow size distribution for CdSe NPs and for both of structures “quantum confinement effect” was observed (Suganthi et al. 2012). The size of CdSe and CdSe/CdS NPs were 2.5 and 5 nm respectively.

There is a focused progress towards the development of controlled synthesis of CdSe nanomaterials of different sizes, shapes, and morphologies. These nanostructures have a number of captivating applications in the field of optoelectronics (Chaudhari et al. 2016), photodetectors (An and Meng 2016), nanosensing (Hooshmand and Es’haghi 2017), biomedical imaging (Li et al. 2016), and high-efficiency solar cells (McElroy et al. 2014). CdSe NPs can be synthesized by different techniques like co-precipitation, electrodeposition (Soundararajan et al. 2009), pulsed sonoelectrochemical (Mastai et al. 1999), solvothermal (Singh et al. 2011) and hot injection method (Williams et al. 2009).

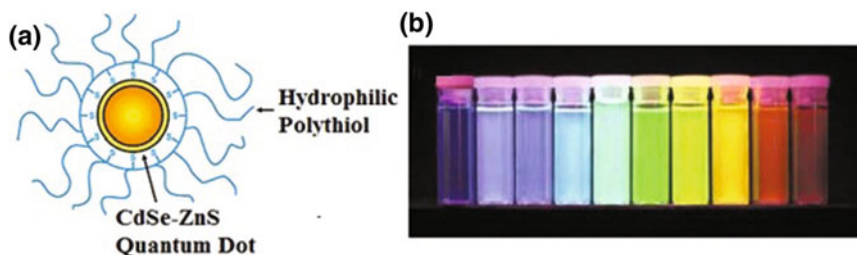


Fig. 2.8 **a** Schematic diagram of hydrophilic polythiol coated CdSe-ZnS QD (Yildiz et al. 2009). © 2009 American Chemical Society **b** The emission of fluorescence colors in ZnS-capped CdSe QDs different-sized CdSe QDs (Han et al. 2001). © 2011 Nature Publishing Group

2.6.4 Cadmium Telluride

Cadmium selenide (CdTe) is a binary compound of cadmium and tellurium. It is a direct band gap semiconductor with a band gap of 1.56 eV, and its nanomaterial has a band gap ranging from 1.5 to 2.1 eV. The thermal conductivity of these nanomaterials makes them suitable for use in thermoelectric applications.

This is comparatively a narrow band gap semiconductor and achieved huge consideration because it covers unique portion of solar spectrum and have a high absorption coefficient which make it an appropriate material for use in photovoltaic devices (Li et al. 2013), light-emitting diodes (Chin et al. 2008), and drug nanocarriers (Wang et al. 2014). CdTe is used as window material for hetero-junction solar cells to avoid the recombination of photo-generated carriers which consequently improves the solar cells efficiency (Morales-Acevedo 2006). CdTe NWs were self-assembled by eliminate the shielding of organic stabilizer

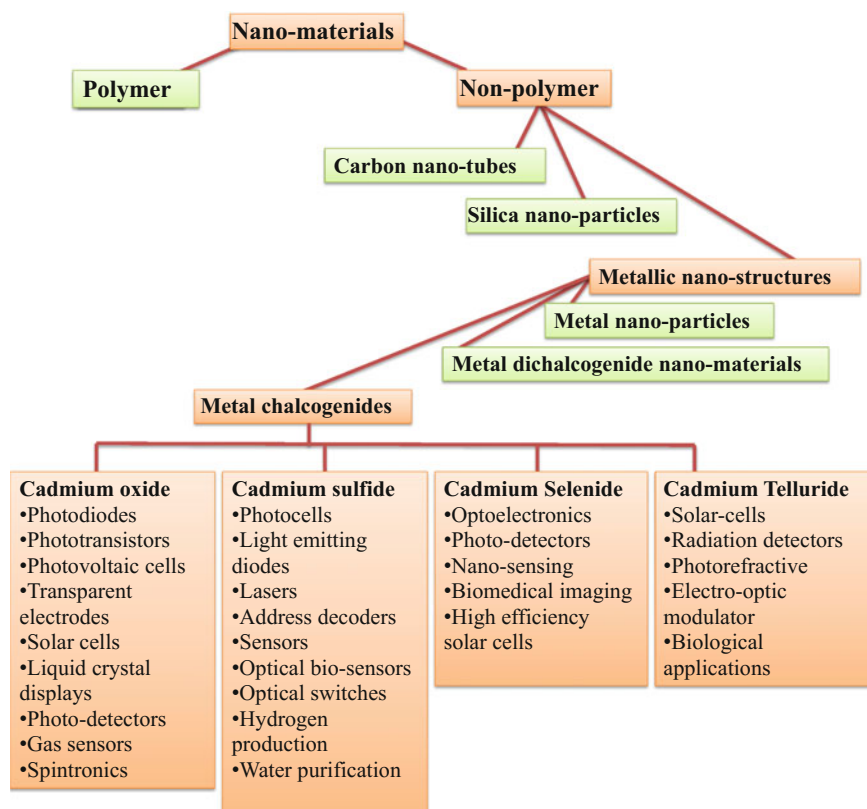


Fig. 2.9 Classification of nanomaterials and applications-tree of cadmium chalcogenide nanomaterials

(Tang et al. 2006). The synthesized NWs have a high aspect ratio, homogeneity, and optical performance (Tang et al. 2002). CdTe nanostructures have been stabilized by the thioglycolic acid. Exclusion of stabilizer is one of the main features to obtain NWs from NPs. CdTe in the form of NWs showed suitable properties to be used in optoelectronic applications (Yang et al. 2010).

In photovoltaics, it has been exploited to fabricate CdTe and copper indium diselenide solar cells to act as a window layer that separates charge carriers produced due to photon absorption and photo detectors (Wang et al. 2006) and in the fabrication of thin film solar cells (Romeo et al. 2007). Crisp et al. has prepared a monolithic CdTe–PbS tandem solar cell structural design with 40% power conversion efficiency (Crisp et al. 2017). CdTe and PbS absorber layers are properly merged in sequence through a ZnTe–ZnO tunnel junction. In medical field, molecular analysis is very significant in determining the progress in health. CdTe QDs immobilized on paper-based sensing device are very potential materials to analyze the beginning and development of disease conditions (Lin et al. 2017). CdTe nanostructures have potential for application in solar cells (Singh et al. 2004), radiation detectors (Toyama et al. 2006), photorefractive (Shcherbin et al. 2002), electro-optic modulator (Taki 2013), and biological (Wang et al. 2005) applications. The classification of nanomaterials and applications of cadmium chalcogenide nanomaterials is sketched in Fig. 2.9.

2.7 Characterization Methods

In order to study the properties of synthesized nanomaterials, a number of characterization techniques are used. A brief description on major experimental techniques used to characterize the nanomaterials is given in the following.

2.7.1 Structural Characterization via X-ray Diffraction

XRD (X-ray diffraction) is a basic and necessary tool for study of structural properties of nanomaterials. It is the most widely used method to investigate the crystal structure, lattice parameters, grain size, and phase of nanomaterials. In order to establish the formation of structural phase of synthesized nanomaterials, it is a primary and non-destructive tool which provides quick and reliable information.

The Bragg positions of the lines on the XRD patron gives information on crystal structure unit cell parameters and related data. The grain size of the nanomaterials is usually obtained from the width of peak and computed by using the Scherrer equation given below;

$$D = \frac{k\lambda}{\beta \cos \theta},$$

where λ = wavelength of X-rays, β = width at half maximum of peaks. D is mean crystalline dimension perpendicular to the reflecting parts. The value of Scherrer constant k depends upon the shape of nanomaterial; for spherical shaped particles, its value is 0.9.

The XRD graph with 2θ (degrees) versus intensity is commonly used to collect basic crystallographic information about the samples. The position, height, width, and shape of the obtained peak are finger prints of the material and can be used to access its structural properties. In order to find these parameters, Gaussian and Lorentz functions are commonly used to analyze single peaks as well as overlapping peaks via multiple curve fitting procedure. For crystallographic analysis of XRD data, several software are available, e.g., X'Pert Highscore, JADE, Match, GSAS, TOPAS, XLENS, DQUANT, etc. Following sections may help in interpretation of XRD results.

Peak position: 2θ values given on x-axis are related to miller indices (hkl) of planes and provide information related to interplanar spacing, lattice constants, etc. The phases identification can be made using peak position. From the obtained XRD patron, chose a peak and find the corresponding Bragg angle θ (by halving the position of the peak) of your sample. Using this angle θ , wavelength of X-rays and order of diffraction, one can easily find d -value of the corresponding phase using Bragg's law $2d\sin\theta = n\lambda$. Similarly, d -values corresponding to all notable peaks can be found which help to index and hence identification of probable phases after comparison with standard phases (using JCPDS for instance).

Peak height: The intensity of peaks given along y-axis shed light on crystallinity, atomic positions, thickness of structural phases etc.

Peak width: Full width of peak at half of maximum intensity (FWHM) gives its width measured usually in degrees. It can be used to find crystallite size, size distribution, micro-strain analysis, etc. The broadening of peak (excluding the chances of instrumental broadening) is inversely proportional to crystallite size and can be used to find the size as per Scherrer equation. For a particular material, if we keep on gradually dividing the crystallite into smaller and smaller grains, the broadening of peak will increase accompanied with decrease in peak height but *in-principle* area under the curve remains constant.

It is worth mentioning that broadening due to grain size, micro-strain, and instrument greatly increase for the higher Bragg angles. At lower Bragg angles, peak symmetry whereas at higher Bragg angles peak height are considered to obtain meaningful results. For comparison purposes, and getting reliable results, it is recommended that data related to intermediate 2θ scale (30–60°) should be preferred.

Peak Shape: The shape of XRD peak is usually ignored but it contains important structural information. The changes in shape of peak at its top and bottom should be considered to shed light on grain size, lattice strain, etc. Sometimes, peak

is found asymmetric (at lower or higher angle sides) which contains important information and should be carefully analyzed.

Determination of Strain: The structural variations (due to issues related to chemical compositions, lattice relaxation, etc.) observed for materials when compared with the bulk point to the presence of strain in the synthesized nanomaterials or thin films. It should be carefully analyzed because the presence of strain in local regions of microstructure changes the material's behavior. The strain may be present in two different modes; (i) The shift in peak position without any change in its broadening points to the presence of homogenous strain in the sample. In this case, every crystallite is strained in same amount which uniformly changes the interplanar spacing throughout. The peak is shifted to higher (lower) angles exhibiting compressive (tensile) strain. (ii) The shift in peak position associated with change in its broadening points to the presence of inhomogeneous strain. The crystallites are non-uniformly strained so every crystallite causes different change in 2θ and hence produces different shift in peak position. The inhomogeneous strain associated with structural defects (point, line, areal, volume, etc.) is calculated via ratio of change in interplanar spacing to the unstrained spacing. The strain evaluation should be carefully monitored because the broadening may also be caused by simultaneous effects of inhomogeneous strain and size which demands more rigorous treatment (e.g., Williamson Hall method).

2.7.2 Surface Morphological Characterization

The investigation of morphology of prepared nanomaterials is very important, since the resulting properties of the product are highly dependent on its size, shape, and structural arrangement. The techniques involving microscopy giving high-resolution images of local areas of samples are used to be employed for this purpose.

2.7.2.1 Scanning Probe Microscopy (SPM)

SPM consists of scheme closely related to STM and AFM. Piezoelectric transducer is used with a pointed probe scanned transversely on the surface; the probes can be placed upon the surface with Angstrom precisions. This provides the capability to investigate the spectroscopic information related even to a single atom.

2.7.2.2 Scanning Tunneling Microscopy (STM)

This method works on the basis of quantum mechanical tunneling phenomenon. Real-space images of the surfaces can be generated with atomic resolution. The

tunneling happens between the atomically pointed metallic tip and the conductive surface of the sample. This characterization method has started the advancement in novel classes of materials.

2.7.2.3 Atomic Force Microscopy (AFM)

AFM is an inexpensive method and is a modification appeared after development of STM (Binnig et al. 1986). In this method, van der Waals forces are mechanically determined between atomically pointed metallic tip and the surface using a flexible cantilever. STM can study the electronic behavior around the surface as well as can manipulate the individual atoms. This method can also be used for several forces like magnetic and electrostatic forces and for the study of chemical interactions. This double ability to investigate the currents and forces at nanometer and atomic scale has initiated a range of scanning probe microscopy (SPM) methods like magnetic force microscopy, electrostatic force microscopy, scanning capacitance microscopy, near-field scanning optical microscopy. These methods offered the potential for study of local, mechanical, optical, electrical, magnetic, thermal, and chemical properties of nanomaterials.

2.7.2.4 Scanning Electron Microscope (SEM)

SEM characterization technique was first time introduced in 1938. This method can offer the extremely magnified images of the surface and near-surface composition of the nanomaterials. Size, shape, microstructure, composition, and grain orientation can be calculated using this technique. The resolution and magnification of SEM can be simply controlled to a small number of nanometers and 10–300,000 times respectively. The working mechanism of this technique involves incidence of a focused electron beam on the surface of material ranging from 50 nm to 1 cm as a result of which electrons hit the surface to produce several signals which are recorded by detectors. These signals obtained from the specimen are then processed and showed on screen of CRO in the form of images. Secondary electron and backscattered electrons produce the images in SEM. The properties of these images are shown in Table 2.4.

2.7.2.5 Transmission Electron Microscopy (TEM)

TEM is the study of ultra-thin specimen through transmission of electrons from it, typical thickness 50–100 nm for beam of 100 keV. It is very costly method with beam of electrons having energy 100,000–400,000 eV. The obtained information is detected and displayed in the form of images onto an imaging device with range 50 nm–500 μm . A TEM consists of a vacuum system, chain of electromagnetic

Table 2.4 Image profiles of SEM

| Properties/ SEM images | Scattering type | Energy | Resolution | Image type | Occurred |
|-------------------------------|--|--------------------|------------|---------------|-------------------------------------|
| Secondary electron images | Inelastic scattering with atomic electrons | Less than 50 eV | High | 3D appearance | Area near the beam impact zone |
| Backscattered electron images | Elastic scattering with atomic nucleus | Greater than 50 eV | – | – | In material with high atomic number |

lenses, additional electrostatic plates, and imaging devices. An electron gun is included for thermionic emission of electrons.

TEM has appeared in diverse forms as high-resolution transmission microscopy (HRTEM), scanning transmission electron microscopy (STEM), etc. Variations in the phases of scattered electron beam show the contrast in TEM images, which provides basis for HRTEM. STEM offers a diverse number of modes to find the electronic structure and elemental composition of atoms. This is similar to SEM, only the specimen used is very thin for providing the transmission modes of imaging. Resolution of TEM depends upon the volume of the specimen, smaller volume shows the higher resolution, and so limitation of volume is a disadvantage of this method. Dimensionality is another problem using TEM, because it displays 2D images of 3D objects.

2.7.2.6 X-ray Photoelectron Spectroscopy (XPS)

This method was initially developed for investigation of composition and stoichiometry of the materials. XPS is a surface-sensitive technique for chemical analysis in which X-rays (high energy photons) are used to eject the core electrons from surface atoms. Study of the kinetic energy of these X-ray photoelectrons is used to determine the properties of the nanomaterials ranging from 1 to 10 nm.

The spectra obtained after XPS of samples gives binding energy (BE) of core shell electrons which can be used to explain the physical process (splitting of multiplets, chemical interactions, etc.) and measurement of material's parameters (chemical environment, ionic charge states, chemical composition, bonding, etc.). This technique is useful for characterization of top 1–10 nm of materials so it is highly sensitive to provide important information in case of nanomaterials.

Careful sample handling (including cleaning), choice of experimental conditions, and correct operation of the spectrometer are prerequisites to obtain reliable spectroscopic results. After conducting XPS of your samples, or upon receiving XPS data from your laboratory staff, the identification of peaks is the step of prime importance. The entire peaks obtained in XPS spectra are not photoelectron signatures of the material but also contain Auger lines, satellite peaks, background

signal, and noise. A careful analysis is required to assign peaks purely related to photoelectrons for measurement of corresponding BE.

Two most important parameters reflected from XPS spectra obtained after ionization of a particular core shell are BE on x -axis and intensity on y -axis. The XPS data processing includes background subtraction (and smoothing, if needed) and peak fitting analysis (using XPSPEAK, CasaXPS, etc.) to perform elemental identification by using NIST data or published literature by considering position of the peaks. The multiple peak fitting helps to deconvolute the overlapping peaks which are sometimes obtained in XPS spectra. It is an important step in which you should anticipate the spectrum by considering the recipe of your sample and the substrate (if any) into account. The interpretation of the spectrum should be carried out by focusing on different aspects of the peaks including position, height, width, shape, etc. The primary information on these features is given below.

Peak position: The peak position gives BE and acts as finger print to obtain information on chemical state of the material. It is at heart of XPS spectroscopy and provides elemental identification based on analysis of orbital's peaks. It should be noted that peaks related to s orbital are in the form of singlets whereas the peaks representing p , d , f orbitals are doublets due to spin-splitting.

Peak height: The intensity points out the amount of material in the scanning region (sample's surface), because number of emitting electrons is proportional to number of atoms therein. If multiple peaks, instead of a single peak, are obtained then relative intensity provide useful information and can be used to estimate the elemental or chemical composition in the surface region. The atomic percentage depends upon relative intensity and is equal to ratio of intensity of relevant peak to cumulative intensity of all peaks by taking sensitivity factor into account.

Peak width: The peak width (FWHM) and change in its value upon sample's processing contains information about chemical environment and change of chemical state of the material. It may help in shedding light on number and nature of chemical bonds. The reasons of broadening include presence of charge, inhomogeneity, vibrational states, etc., of the samples.

Peak shape: The changes in peak shape points to surface modification of samples and appearance of charge upon processing or X-ray irradiation. The asymmetry in the form of tailing of BE curves on higher energy side is often found in case of metals, metallic compounds, or metals doped semiconductor/insulators. It contains important information and should be carefully analyzed by suitable choice of fitting function.

2.7.2.7 Auger Electron Spectroscopy (AES)

AES method was proposed in 1925 when Auger observed that due to the X-rays or high energy irradiation, the ionized atom can eject one more electron. The first emitted electron must be from inner shells to eject another electron from surface known as auger electron. This second emitted electron is used to investigate the

material properties by calculating its kinetic energy. As in XPS, AES can also determine the 10 nm of the material's surface and used to recognize the elements in the material. The value of resolution of AES is 10 nm with sensitivity of about 0.3% higher than XPS.

2.7.3 *Optical Characterization Techniques*

There are a number of techniques used for optical characterization of prepared nanomaterials. These techniques are mostly quick, reliable, and non-destructive. These are available in several configurations and several research groups used home built equipment for the purpose.

2.7.3.1 UV-Vis Spectroscopy

This is a comparatively simple and efficient method to observe the characteristic absorption edges and band gap of the materials. It is also used to find the concentration of components of organic and inorganic nanomaterials and recognize the functional groups in the substances. Ultra-violet and visible range electromagnetic radiations are used to quantitatively study the materials ranging from 400 nm to 1 nm and analyze through their absorption spectra. The broadening of the absorption peak tells about the composition, quality, and size distribution of the nanomaterials. Electronic properties like band gap and size-dependent properties like peak broadening and shifts in absorption spectra at nanoscales can also be measured.

UV-Vis spectroscopy can be used to characterize the nanomaterials for determination of concentration, size, distribution, band gap, and several optical properties. It is employed to measure the sample's response (in terms of absorbance, reflectance, transmittance) by shining light in UV and visible regions of electromagnetic spectrum. Generally, it is used in absorbance mode to provide information on the extent of absorption of light (intensity along y -axis) as a function of wavelength or energy (along x -axis) of incident photons.

Not every wavelength will be absorbed by the sample but the absorption will only happen when energy of incident photon matches with energy difference (band gap) of accessible electronic states. When incident energy matches the band gap, an electron in highest occupied energy level (HOMO in case of molecular and VB in case of solids) jumps to lowest unoccupied energy level (LUMO in case of molecular and CB in case of solids) to produce a peak or band in absorption spectrum. The graph gives broad peaks or bands giving spectrum of absorbed radiations and often displays maximum absorbance at certain wavelength.

Band gap determination: In case of insulating or semiconducting samples, HOMO-LUMO gap (for molecular) or band gap (VB-CB difference for solids) can

be straightforwardly measured by observing major absorption peak or absorption edge in the spectrum. Sometimes the peak or the edge shifts to higher energies (blue shift) or lower energies (red shift) due to band gap modifications upon processing of the as-grown sample (alloying, doping, annealing, etc.) which can be easily determined using this technique.

The calculation of band gap of thin films, using data from UV–Vis spectroscopy, involves calculation of absorption coefficient and drawing Tauc plot. However, surface and size effects dominating in case of nanoparticles and film thickness usually does not matter due to which modified procedures are needed to measure the band gap. The fitting of absorption spectrum (Ghobadi 2013) can be used to evaluate the optical band gap of nanomaterials as per following equation;

$$\text{Abs.}(\lambda) = B_1 \lambda \left(\frac{1}{\lambda} - \frac{1}{\lambda_g} \right)^m + B_2,$$

where B_1 and B_2 are constants. Plot a graph of $\left[\frac{\text{Abs.}(\lambda)}{\lambda} \right]^{1/m}$ as a function of $\frac{1}{\lambda}$ and extrapolate the linear portion of the curve (or drop a tangent) to intersect x -axis which will be the value of λ_g after which value of optical band gap can be found by using $E_g = \left(\frac{1240}{\lambda(\text{nm})} \right) \text{eV}$. The value of fitting parameter m points towards direct (with $m = 1/2$) and indirect (with $m = 2$) nature of the optical band gap.

Intensity or Absorbance: The absorbance plotted along y -axis gives ratio of transmitted to incident light and reveals relative number of photons absorbed by the structure which depends upon the concentration of structural units of the material. The comparison of peak intensities in a spectrum helps finding the transition probability for the electronic transitions involved in the process. The absorbance can be translated to the dimensions of the samples by measuring *optical density* which is ratio of absorbance to film thickness (in case of thin films).

Quantum confinement effects: In case of semiconducting nanomaterials, absorption spectrum changes with size of nanomaterial when the size becomes smaller than exciton Bohr radius of the material. Therefore, as the size of nanomaterial decreases the absorption peak shifts to higher energies and this size dependence is known as quantum confinement effect.

2.7.3.2 Photoluminescence (PL) Spectroscopy

It is contactless, non-destructive method which utilizes the electromagnetic radiations usually from laser source to study the luminescent properties of the materials. Many material properties like band gap, impurity levels and recombination mechanism can be determined from intensity, wavelength, peak's width, and stability.

2.7.4 *Vibrational Characterization Techniques*

The study of vibrational properties is often carried out to study lattice vibrational and bonding details of the materials. This class of investigation gives key information of materials to provide reliable information.

2.7.4.1 **Vibrational Spectroscopy**

Vibrational spectroscopy is the study of radiation-matter interaction through vibrational excitation and de-excitation. Vibrational spectroscopy is used for structural study, chemical bonds in the detecting materials, multicomponent qualitative, and quantitative analysis. Vibrational properties of molecules can be studied using the Infrared and Fourier transform infrared spectroscopy technique. **IR and Raman** spectroscopy are examples of vibrational spectroscopy.

2.7.4.2 **Raman Spectroscopy**

This method is used in materials characterization to investigate the vibrational, rotational, and other low-frequency modes.

2.7.4.3 **IR Spectroscopy**

IR spectroscopy is the analysis of interaction of IR radiations with the materials. It is a popular and versatile characterization method based on the vibrations of the atoms and molecules. It is used to study the attachment of organic ligands to organic/inorganic NPs. IR spectrum is determined by examining the sample through a continuous series of IR wavelength as from 400 to 4000 cm^{-1} . IR photons are irradiated to the molecules each have its exclusive nature and their bond type is recognized. Chemical bonds can be turned to many ways: stretching, scissoring, rocking, wagging, and twisting. Almost all organic materials absorb the IR radiations, but inorganic materials are not usually investigated as their peak intensities possibly too weak to be determined. In this method, almost any sample in almost any condition can be characterized. From their results in absorption spectra, the values of energy showing the peaks indicate the vibrational frequencies of that part of the sample.

In IR spectra, peak position, intensity, and width tells about the structure of molecules, concentration of the molecules, and sensitivity for chemical medium (hydrogen bonding and pH) of samples respectively (Suart 2004). This method is comparatively fast, easy, low-cost and almost a universal characterization method. However, there are some disadvantages like it cannot detect some molecules. If the sample is more complicated, then the spectral peaks are so mixed that they cannot be distinguished from each other.

2.7.4.4 Fourier Transform Infrared (FTIR) Spectroscopy

FTIR spectroscopy is the specific form of IR spectrometry with advanced qualities of IR characterization method. It is used to study the molecular vibrations and resonance study (Smith 2011). IR photons are produced from a blackbody source. The interferometer is used to encode these photons resulting in the form of signals. These signals are transmitted to or reflected off the surface of the sample. Then these signals are perceived by specially designed detector for further processing. Analog to digital conversion is performed and the digital signals are sent to computer. Fourier transform carried out in computer and the FTIR spectrum is obtained.

This method is very fast and the measurements are made in seconds. There are many frequencies which can be measured at the same time using this method. Signal-to-noise ratio (SNR = signal/noise) determines the quality of the peak. Signal is the measure of size of the peak, while noise is the error. In comparison to IR, FTIR provides an advantage of measuring a high value of SNR and 10–100 times better than IR spectrometers.

References

- Acharya, K. P. (2009). *Photocurrent spectroscopy of CdS/plastic, CdS/glass, and ZnTe/GaAs hetero-pairs formed with pulsed-laser deposition* (Doctoral dissertation, Bowling Green State University).
- Acharya, A., Sahu, S., Balamurgan, S., & Roy, G. S. (2011). Effect of doping on nano cadmium-selenide (CdSe)-assessment through UV-VIS spectroscopy. *Latin American Journal of Physics Education*, 5(1), 134.
- Afify, H. H., Ahmed, N. M., Tadros, M. Y., & Ibrahim, F. M. (2014). Temperature dependence growth of CdO thin film prepared by spray pyrolysis. *Journal of Electrical Systems and Information Technology*, 1(2), 119–128.
- Aldwayyan, A. S., Al-Jekhedab, F., Al-Noaimi, M., Hammouti, B., Hadda, T. B., Suleiman, M., et al. (2013). Synthesis and characterization of CdO NPs starting from organometallic dmphen-CdI₂ complex. *International Journal of Electrochemical Science*, 8(10506), e10514.
- Alemi, A., Joo, S. W., Khademinia, S., Dolatyari, M., Bakhtiari, A., Moradi, H., et al. (2013). Sol-gel synthesis, characterization, and optical properties of Gd³⁺-doped CdO sub-micron materials. *International Nano Letters*, 3(1), 1.
- Alivisatos, A. P. (1996). Perspectives on the physical chemistry of semiconductor NCs. *The Journal of Physical Chemistry*, 100(31), 13226–13239.
- Amiri, G. R., Fatahian, S., & Mahmoudi, S. (2013). Preparation and optical properties assessment of cdse QDs. *Materials Sciences and Applications*, 4(02), 134.
- An, Q., & Meng, X. (2016). Aligned arrays of CdS NTs for high-performance fully nanostructured photodetector with higher photosensitivity. *Journal of Materials Science: Materials in Electronics*, 27(11), 11952–11960.
- Aqra, F., & Ayyad, A. (2014). Surface free energy of alkali and transition metal NPs. *Applied Surface Science*, 314, 308–313.
- Arora, S., & Manoharan, S. S. (2007). Size-dependent photoluminescent properties of uncapped CdS particles prepared by acoustic wave and microwave method. *Journal of Physics and Chemistry of Solids*, 68(10), 1897–1901.

- Balamurugan, S., Balu, A. R., Usharani, K., Suganya, M., Anitha, S., Prabha, D., et al. (2016). Synthesis of CdO nanopowders by a simple soft chemical method and evaluation of their antimicrobial activities. *Pacific Science Review A: Natural Science and Engineering*, 18(3), 228–232.
- Banerjee, R., Jayakrishnan, R., & Ayyub, P. (2000). Effect of the size-induced structural transformation on the band gap in CdS NPs. *Journal of Physics: Condensed Matter*, 12(50), 10647.
- Baranov, A. M., Malov, Y. A., Teryoshin, S. A., & Val'dner, V. O. (1997). Investigation of the properties of CdO films. *Technical Physics Letters*, 23(10), 805–806.
- Benhaliliba, M., Benouis, C. E., Tiburcio-Silver, A., Yakuphanoglu, F., Avila-Garcia, A., Tavira, A., et al. (2012). Luminescence and physical properties of copper doped CdO derived nanostructures. *Journal of Luminescence*, 132(10), 2653–2658.
- Binnig, G., Quate, C. F., & Gerber, C. (1986). Atomic force microscope. *Physical Review Letters*, 56(9), 930.
- Brock, S. L. (2004). *Nanostructures and nano-materials: Synthesis, properties and applications By Guozhang Cao (University of Washington) (434 pp.)*. London: Imperial College Press (distributed by World Scientific). ISBN 1-86094-415-9.
- Buhro, W. E., & Colvin, V. L. (2003). Semiconductor NCs: Shape matters. *Nature Materials*, 2(3), 138–139.
- Cao, G. (2004). *Nanostructures and nanomaterials: Synthesis, properties and applications*. World Scientific.
- Cao, G., & Liu, D. (2008). Template-based synthesis of nanorod, nanowire, and nanotube arrays. *Advances in Colloid and Interface Science*, 136(1), 45–64.
- Chaudhari, K. B., Gosavi, N. M., Deshpande, N. G., & Gosavi, S. R. (2016). Chemical synthesis and characterization of CdSe thin films deposited by SILAR technique for optoelectronic applications. *Journal of Science: Advanced Materials and Devices*, 1(4), 476–481.
- Chauré, S. (2016). Synthesis and characterization of vertically aligned cadmium oxide nanowire array. *Journal of Materials Science: Materials in Electronics*, 2(28), 1832–1836.
- Chen, C. C., Herhold, A. B., Johnson, C. S., & Alivisatos, A. P. (1997). Size dependence of structural metastability in semiconductor NCs. *Science*, 276(5311), 398–401.
- Chin, P. T., Stouwdam, J. W., van Bavel, S. S., & Janssen, R. A. (2008). Cluster synthesis of branched CdTe NCs for use in light-emitting diodes. *Nanotechnology*, 19(20), 205602.
- Crisp, R. W., Pach, G. F., Kurley, J. M., France, R. M., Reese, M. O., Nanayakkara, S. U., et al. (2017). Tandem solar cells from solution-processed CdTe and PbS QDs using a ZnTe–ZnO tunnel junction. *Nano Letters*, 17(2), 1020–1027.
- Dagdelen, F., Serbetci, Z., Gupta, R. K., & Yakuphanoglu, F. (2012). Preparation of nanostructured Bi-doped CdO thin films by sol–gel spin coating method. *Materials Letters*, 80, 127–130.
- Dai, G., Zou, B., & Wang, Z. (2010). Preparation and periodic emission of superlattice CdS/CdS: SnS₂ microwires. *Journal of the American Chemical Society*, 132(35), 12174–12175.
- Dakhel, A. A. (2011a). Effect of cerium doping on the structural and optoelectrical properties of CdO nanocrystallite thin films. *Materials Chemistry and Physics*, 130(1), 398–402.
- Dakhel, A. A. (2011b). Effect of thermal annealing in different gas atmospheres on the structural, optical, and electrical properties of Li-doped CdO nanocrystalline films. *Solid State Sciences*, 13(5), 1000–1005.
- Dakhel, A. A. (2012). Structural and optoelectronic properties of Zn-incorporated CdO films prepared by sol–gel method. *Journal of Alloys and Compounds*, 539, 26–31.
- Djurišić, A. B., & Leung, Y. H. (2006). Optical properties of ZnO nanostructures. *Small*, 2(8–9), 944–961.
- Duan, X., Huang, Y., Agarwal, R., & Lieber, C. M. (2003). Single-nanowire electrically driven lasers. *Nature*, 421(6920), 241–245.
- El-Baz, A. F., Sorour, N. M., & Shetaia, Y. M. (2016). Trichosporon jirovecii-mediated synthesis of cadmium sulfide NPs. *Journal of Basic Microbiology*, 56(5), 520–530.

- Fox, M. (2002). *Optical properties of solids. Oxford Master Series in Condensed Matter Physics*. New York: Oxford University Press.
- Gao, X. F., Li, H. B., Sun, W. T., Chen, Q., Tang, F. Q., & Peng, L. M. (2009). CdTe QDs-sensitized TiO₂ nanotube array photoelectrodes. *The Journal of Physical Chemistry C*, 113(18), 7531–7535.
- Ge, M., Li, Q., Cao, C., Huang, J., Li, S., Zhang, S., ... & Lai, Y. (2016). One-dimensional TiO₂ nanotube photocatalysts for solar water splitting. *Advanced science*.
- Ghobadi, N. (2013). Band gap determination using absorption spectrum fitting procedure. *International Nano Letters*, 3(1), 2.
- Ghoshal, T., Biswas, S., Nambissan, P. M. G., Majumdar, G., & De, S. K. (2009). Cadmium oxide octahedrons and NWs on the micro-octahedrons: A simple solvothermal synthesis. *Crystal Growth & Design*, 9(3), 1287–1292.
- Goldstein, A. N., Echer, C. M., & Alivisatos, A. P. (1992). Melting in semiconductor NCs. *Science*, 256(5062), 1425–1427.
- Goswami, B., & Choudhury, A. (2015). Enhanced visible luminescence and modification in morphological properties of cadmium oxide NPs induced by annealing. *Journal of Experimental Nanoscience*, 10(12), 900–910.
- Guo, Z., & Tan, L. (2009). *Fundamentals and applications of nanomaterials*. Norwood: Artech House.
- Gupta, R. K., Ghosh, K., Patel, R., & Kahol, P. K. (2008). Effect of oxygen partial pressure on structural, optical and electrical properties of titanium-doped CdO thin films. *Applied Surface Science*, 255(5), 2414–2418.
- Han, M., Gao, X., Su, J. Z., & Nie, S. (2001). Quantum-dot-tagged microbeads for multiplexed optical coding of biomolecules. *Nature Biotechnology*, 19(7), 631.
- Harrell, S. M., McBride, J. R., & Rosenthal, S. J. (2013). Synthesis of ultrasmall and magic-sized CdSe NCs. *Chemistry of Materials*, 25(8), 1199–1210.
- He, X., & Ma, N. (2014). An overview of recent advances in QDs for biomedical applications. *Colloids and Surfaces B: Biointerfaces*, 124, 118–131.
- Hooshmand, S., & Es' hagh, Z. (2017). Microfabricated disposable nanosensor based on CdSe quantum dot/ionic liquid-mediated hollow fiber-pencil graphite electrode for simultaneous electrochemical quantification of uric acid and creatinine in human samples. *Analytica Chimica Acta*, 972, 28–37.
- Hu, D., Zhang, P., Gong, P., Lian, S., Lu, Y., Gao, D., et al. (2011). A fast synthesis of near-infrared emitting CdTe/CdSe QDs with small hydrodynamic diameter for in vivo imaging probes. *Nanoscale*, 3(11), 4724–4732.
- Hu, L., Choi, J. W., Yang, Y., Jeong, S., La Mantia, F., Cui, L. F., et al. (2009). Highly conductive paper for energy-storage devices. *Proceedings of the National Academy of Sciences*, 106(51), 21490–21494.
- Huang, L., Lin, C. C., Riediger, M., Röder, R., Tse, P. L., Ronning, C., et al. (2015). Nature of AX Centers in Antimony-Doped Cadmium Telluride NBs. *Nano Letters*, 15(2), 974–980.
- Jefferson, P. H., Hatfield, S. A., Veal, T. D., King, P. D. C., McConville, C. F., Zúñiga-Pérez, J., et al. (2008). Bandgap and effective mass of epitaxial cadmium oxide. *Applied Physics Letters*, 92(2), 022101.
- Jimenez-Perez, J. L., Fuentes, R. G., Sánchez-Sosa, R., Torres, M. Z., Correa-Pacheco, Z. N., & Ramirez, J. S. (2015). Thermal diffusivity study of NPs and NRs of titanium dioxide (TiO₂) and titanium dioxide coated with cadmium sulfide (TiO₂ 2 CdS). *Materials Science in Semiconductor Processing*, 37, 62–67.
- Kalhor, H., Irajizad, A., Azarian, A., & Ashiri, R. (2015). Synthesis and characterization of electrochemically grown CdSe NWs with enhanced photoconductivity. *Journal of Materials Science: Materials in Electronics*, 26(3), 1395–1402.
- Kamarudin, S. K., Achmad, F., & Daud, W. R. W. (2009). Overview on the application of direct methanol fuel cell (DMFC) for portable electronic devices. *International Journal of Hydrogen Energy*, 34(16), 6902–6916.

- Kamat, P. V. (2008). Quantum dot solar cells. Semiconductor NCs as light harvesters. *The Journal of Physical Chemistry C*, 112(48), 18737–18753.
- Kargar, A., Sun, K., Jing, Y., Choi, C., Jeong, H., Jung, G. Y., et al. (2013). 3D branched nanowire photoelectrochemical electrodes for efficient solar water splitting. *ACS Nano*, 7(10), 9407–9415.
- Khalily, M. A., Eren, H., Akbayrak, S., Susapto, H. H., Biyikli, N., Özkaz, S., et al. (2016). Facile synthesis of three-dimensional Pt-TiO₂ nano-networks: A highly active catalyst for the hydrolytic dehydrogenation of ammonia-borane. *Angewandte Chemie*, 128(40), 12445–12449.
- Khan, A., Khan, R., Waseem, A., Iqbal, A., & Shah, Z. H. (2016). CdS nanocapsules and nanospheres as efficient solar light-driven photocatalysts for degradation of Congo red dye. *Inorganic Chemistry Communications*, 72, 33–41.
- Kim, W., Baek, M., & Yong, K. (2016). Fabrication of ZnO/CdS, ZnO/CdO core/shell nanorod arrays and investigation of their ethanol gas sensing properties. *Sensors and Actuators B: Chemical*, 223, 599–605.
- Krishnakumar, T., Jayaprakash, R., Prakash, T., Sathiyaraj, D., Donato, N., Licoccia, S., et al. (2011). CdO-based nanostructures as novel CO₂ gas sensors. *Nanotechnology*, 22(32), 325501.
- Li, D., Wang, S., Wang, J., Zhang, X., & Liu, S. (2013). Synthesis of CdTe/TiO₂ 2 NPs and their photocatalytic activity. *Materials Research Bulletin*, 48(10), 4283–4286.
- Li, L., Abild-Pedersen, F., Greeley, J., & Nørskov, J. K. (2015). Surface tension effects on the reactivity of metal NPs. *The Journal of Physical Chemistry letters*, 6(19), 3797–3801.
- Li, L., Yang, S., Han, F., Wang, L., Zhang, X., Jiang, Z., et al. (2014). Optical sensor based on a single CdS nanobelt. *Sensors*, 14(4), 7332–7341.
- Li, X., Jia, Y., Wei, J., Zhu, H., Wang, K., Wu, D., et al. (2010). Solar cells and light sensors based on nanoparticle-grafted carbon nanotube films. *ACS Nano*, 4(4), 2142–2148.
- Li, Y., Zhang, J., Guo, Y., Chen, M., Wang, L., Sun, R., et al. (2016). Cellulosic micelles as nanocapsules of liposoluble CdSe/ZnS QDs for bioimaging. *Journal of Materials Chemistry B*, 4(39), 6454–6461.
- Lin, C. F., Liang, E. Z., Shih, S. M., & Su, W. F. (2002, June). CdS nanoparticle light-emitting diode on Si. In *Symposium on Integrated Optoelectronic Devices* (pp. 102–110). International Society for Optics and Photonics.
- Lin, S. X., Wong, M. M. K., Pat, P. K., Wong, C. Y., Chiu, S. K., & Pun, E. Y. B. (2013, May). Optical biosensor based on cadmium sulfide-silver nanoplate hybrid structure. In *Proc. of SPIE Vol* (Vol. 8774, pp. 877413–1).
- Lin, Z., Lv, S., Zhang, K., & Tang, D. (2017). Optical transformation of a CdTe quantum dot-based paper sensor for a visual fluorescence immunoassay induced by dissolved silver ions. *Journal of Materials Chemistry B*, 5(4), 826–833.
- Liu, J. W., Chen, F., Zhang, M., Qi, H., Zhang, C. L., & Yu, S. H. (2010). Rapid microwave-assisted synthesis of uniform ultralong Te NWs, optical property, and chemical stability. *Langmuir*, 26(13), 11372–11377.
- Liu, X., Li, C., Han, S., Han, J., & Zhou, C. (2003). Synthesis and electronic transport studies of CdO nanoneedles. *Applied Physics Letters*, 82(12), 1950–1952.
- Lopes, P. A., Santos, M. B., Mascarenhas, A. J. S., & Silva, L. A. (2014). Synthesis of CdS nano-spheres by a simple and fast sonochemical method at room temperature. *Materials Letters*, 136, 111–113.
- Lu, H. B., Liao, L., Li, H., Tian, Y., Wang, D. F., Li, J. C., et al. (2008). Fabrication of CdO NTs via simple thermal evaporation. *Materials Letters*, 62(24), 3928–3930.
- Lu, Q., Gao, F., & Komarneni, S. (2004). Microwave-assisted synthesis of one-dimensional nanostructures. *Journal of Materials Research*, 19(6), 1649–1655.
- Luo, B., Liu, G., & Wang, L. (2016). Recent advances in 2D materials for photocatalysis. *Nanoscale*, 8(13), 6904–6920.
- Ma, J., Lian, J., Duan, X., Liu, Z., Peng, P., Liu, X., et al. (2011). Growth of tellurium nanowire bundles from an ionic liquid precursor. *CrystEngComm*, 13(7), 2774–2778.

- Mahdi, M. A., Hassan, J. J., Ng, S. S., & Hassan, Z. (2013). High-quality ZnCdS nanosheets prepared using solvothermal synthesis. *Journal of Nanoscience*, 2013.
- Majid, A., Arshad, H., & Murtaza, S. (2015). Synthesis and characterization of Cr doped CdSe NPs. *Superlattices and Microstructures*, 85, 620–623.
- Mastai, Y., Polsky, R., Koltypin, Y., Gedanken, A., & Hodes, G. (1999). Pulsed sonoelectrochemical synthesis of cadmium selenide NPs. *Journal of the American Chemical Society*, 121(43), 10047–10052.
- Mayers, B., & Xia, Y. (2002a). Formation of tellurium NTs through concentration depletion at the surfaces of seeds. *Advanced Materials*, 14(4), 279–282.
- Mayers, B., & Xia, Y. (2002b). One-dimensional nanostructures of trigonal tellurium with various morphologies can be synthesized using a solution-phase approach. *Journal of Materials Chemistry*, 12(6), 1875–1881.
- McElroy, N., Page, R. C., Espinbarro-Valazquez, D., Lewis, E., Haigh, S., O'Brien, P., et al. (2014). Comparison of solar cells sensitized by CdTe/CdSe and CdSe/CdTe core/shell colloidal QDs with and without a CdS outer layer. *Thin Solid Films*, 560, 65–70.
- Mews, A., Eychmüller, A., Giersig, M., Schooss, D., & Weller, H. (1994). Preparation, characterization, and photophysics of the quantum dot quantum well system cadmium sulfide/mercury sulfide/cadmium sulfide. *The Journal of Physical Chemistry*, 98(3), 934–941.
- Morales-Acevedo, A. (2006). Can we improve the record efficiency of CdS/CdTe solar cells? *Solar Energy Materials and Solar Cells*, 90(15), 2213–2220.
- Moras, J. D., Strandberg, B., Suc, D., & Wilson, K. (1996). Semiconductor clusters, NCs, and QDs. *Science*, 271, 933.
- Murai, H., Abe, T., Matsuda, J., Sato, H., Chiba, S., & Kashiwaba, Y. (2005). Improvement in the light emission characteristics of CdS: Cu/CdS diodes. *Applied Surface Science*, 244(1), 351–354.
- Murugadoss, G., Thangamuthu, R., Jayavel, R., & Kumar, M. R. (2015). Narrow with tunable optical band gap of CdS based core shell NPs: applications in pollutant degradation and solar cells. *Journal of Luminescence*, 165, 30–39.
- Nozik, A. J. (2002). Quantum dot solar cells. *Physica E: Low-dimensional Systems and Nanostructures*, 14(1), 115–120.
- Ortega, M., Santana, G., & Morales-Acevedo, A. (2000). Optoelectronic properties of CdO/Si photodetectors. *Solid-State Electronics*, 44(10), 1765–1769.
- Plaza, D. O., Gallardo, C., Straub, Y. D., Bravo, D., & Pérez-Donoso, J. M. (2016). Biological synthesis of fluorescent NPs by cadmium and tellurite resistant Antarctic bacteria: exploring novel natural nanofactories. *Microbial Cell Factories*, 15(1), 76.
- Pokropivny, V. V., & Skorokhod, V. V. (2007). Classification of nanostructures by dimensionality and concept of surface forms engineering in nanomaterial science. *Materials Science and Engineering C*, 27(5), 990–993.
- Qi, H., Glembocki, O. J., & Prokes, S. M. (2012). Plasmonic properties of vertically aligned nanowire arrays. *Journal of Nanomaterials*, 2012, 1.
- Qu, L., & Peng, X. (2002). Control of photoluminescence properties of CdSe NCs in growth. *Journal of the American Chemical Society*, 124(9), 2049–2055.
- Radi, P. A., Brito-Madurro, A. G., Madurro, J. M., & Dantas, N. O. (2006). Characterization and properties of CdO NCs incorporated in polyacrylamide. *Brazilian Journal of Physics*, 36(2A), 412–414.
- Rajesh, N., Kannan, J. C., Leonardi, S. G., Neri, G., & Krishnakumar, T. (2014). Investigation of CdO nanostructures synthesized by microwave assisted irradiation technique for NO₂ gas detection. *Journal of Alloys and Compounds*, 607, 54–60.
- Rajeshwar, K., de Tacconi, N. R., & Chenthamarakshan, C. R. (2001). Semiconductor-based composite materials: Preparation, properties, and performance. *Chemistry of Materials*, 13(9), 2765–2782.
- Ranjithkumar, R., Irudayaraj, A. A., Jayakumar, G., Raj, A. D., Karthick, S., & Vinayagamoorthy, R. (2016). Synthesis and properties of CdO and Fe doped CdO NPs. *Materials Today: Proceedings*, 3(6), 1378–1382.

- Rathinamala, I., Pandiarajan, J., Jeyakumaran, N., & Prithivikumaran, N. (2014). Synthesis and physical properties of nanocrystalline CdS thin films-influence of sol aging time & annealing temperature. *International Journal of Thin Films Science and Technology*, 3(3), 113–120.
- Romeo, N., Bosio, A., Mazzamuto, S., Romeo, A., & Vaillant-Roca, L. (2007, September). High efficiency CdTe/CdS thin film solar cells with a novel back contact. In *Proceedings of 22nd European Photovoltaic Solar Energy Conference, Milan, Italy* (pp. 3–7).
- Salem, A., Saion, E., Al-Hada, N. M., Kamari, H. M., Shaari, A. H., Abdullah, C. A. C., et al. (2017). Synthesis and characterization of CdSe NPs via thermal treatment technique. *Results in Physics*, 7, 1556–1562.
- Samarasekara, P., & Madushan, P. A. S. (2016). Structural and electrical properties of CdS thin films spin coated on glass substrates. *arXiv preprint arXiv:1606.02435*.
- Senthilvelan, S. (2017). Morphology convenient flower like nanostructures of CdO-SiO₂ nanomaterial and its photocatalytic application. *World Scientific News*, 62, 46–63.
- Shang, L., Tong, B., Yu, H., Waterhouse, G. I., Zhou, C., Zhao, Y., ... & Zhang, T. (2016). CdS nanoparticle-decorated Cd nanosheets for efficient visible light-driven photocatalytic hydrogen evolution. *Advanced Energy Materials*, 6(3).
- Shcherbin, K., Shumelyuk, O., Odoulov, S., & Kratzig, E. (2002, May). Spectrum of the photorefractive CdTe: Ge response in the near infrared. In *Lasers and Electro-Optics, 2002. CLEO '02. Technical Digest. Summaries of Papers Presented at the* (pp. 208–209). IEEE.
- Shi, Q., Cha, Y., Song, Y., Lee, J. I., Zhu, C., Li, X., et al. (2016). 3D graphene-based hybrid materials: Synthesis and applications in energy storage and conversion. *Nanoscale*, 8(34), 15414–15447.
- Singh, J., Lotey, G. S., & Verma, N. K. (2011). Structural, optical and magnetic properties of Cr-doped CdSe NPs. *Digest J Nanomaterd Biostruct*, 6, 1733–1740.
- Singh, R. S., Rangari, V. K., Sanagapalli, S., Jayaraman, V., Mahendra, S., & Singh, V. P. (2004). Nano-structured CdTe, CdS and TiO₂ for thin film solar cell applications. *Solar Energy Materials and Solar Cells*, 82(1), 315–330.
- Singh, V., & Chauhan, P. (2009). Synthesis and structural properties of wurtzite type CdS NPs. *Chalcogenide Letters*, 6(8), 421–426.
- Smith, B. C. (2011). *Fundamentals of fourier transform infrared spectroscopy*. Boca Raton: CRC press.
- Soundararajan, D., Yoon, J. K., Kim, Y. I., Kwon, J. S., Park, C. W., Kim, S. H., et al. (2009). Vertically aligned CdSe and Zn-doped CdSe nanorod arrays grown directly on FTO coated glass: synthesis and characterization. *International Journal of Electrochemical Science*, 4(6), 1628–1637.
- Soylu, M., & Kader, H. S. (2016). Photodiode based on CdO thin films as electron transport layer. *Journal of Electronic Materials*, 11(45), 5756–5763.
- Suart, B. (2004). Infrared spectroscopy: Fundamental and applications.
- Suganthi, A. B., Joshi, A. G., & Sagayaraj, P. (2012). A novel two-phase thermal approach for synthesizing CdSe/CdS core/shell nanostructure. *Journal of Nanoparticle Research*, 14(2), 691.
- Sujitha, V., Murugan, K., Dinesh, D., Pandiyan, A., Aruliah, R., Hwang, J. S., et al. (2017). Green-synthesized CdS nano-pesticides: Toxicity on young instars of malaria vectors and impact on enzymatic activities of the non-target mud crab *Scylla serrata*. *Aquatic Toxicology*, 188, 100–108.
- Sun, Z., Kim, J. H., Zhao, Y., Bijarbooneh, F., Malgras, V., Lee, Y., et al. (2011). Rational design of 3D dendritic TiO₂ nanostructures with favorable architectures. *Journal of the American Chemical Society*, 133(48), 19314–19317.
- Suresh, S. (2013). Studies on the dielectric properties of CdS NPs. *Applied Nanoscience*, 4(3), 325.
- Tadjarodi, A., Imani, M., Kerdari, H., Bijanzad, K., Khaledi, D., & Rad, M. (2014). Preparation of CdO rhombus-like nanostructure and its photocatalytic degradation of azo dyes from aqueous solution. *Nanomaterials and Nanotechnology*, 4, 16.

- Takahashi, T., Nichols, P., Takei, K., Ford, A. C., Jamshidi, A., Wu, M. C., et al. (2012). Contact printing of compositionally graded $\text{CdS}_x\text{Se}_{1-x}$ nanowire parallel arrays for tunable photodetectors. *Nanotechnology*, 23(4), 045201.
- Taki, M. (2013). Structural and optical properties of cadmium telluride $\text{Cd}_x\text{Te}_{1-x}$ thin film by evaporate. *International Journal of Application or Innovation in Engineering & Management*, 2(5), 413–417.
- Tang, X., Hsieh, C., Ou, F., & Ho, S. T. (2015). Ohmic contact of indium oxide as transparent electrode to n-type indium phosphide. *RSC Advances*, 5(29), 22685–22691.
- Tang, Z. R., Yin, X., Zhang, Y., & Xu, Y. J. (2013). Synthesis of titanate nanotube–CdS nanocomposites with enhanced visible light photocatalytic activity. *Inorganic Chemistry*, 52(20), 11758–11766.
- Tang, Z., Kotov, N. A., & Giersig, M. (2002). Spontaneous organization of single CdTe NPs into luminescent NWs. *Science*, 297(5579), 237–240.
- Tang, Z., Zhang, Z., Wang, Y., Glotzer, S. C., & Kotov, N. A. (2006). Self-assembly of CdTe NCs into free-floating sheets. *Science*, 314(5797), 274–278.
- Thema, F. T., Beukes, P., Gurib-Fakim, A., & Maaza, M. (2015). Green synthesis of Montepontite CdO NPs by Agathosma betulina natural extract. *Journal of Alloys and Compounds*, 646, 1043–1048.
- Thirsk, H. R. (1989). Electrochemistry. In *Royal Society of Chemistry* (Vol. 7).
- Thovhogi, N., Park, E., Manikandan, E., Maaza, M., & Gurib-Fakim, A. (2016). Physical properties of CdO NPs synthesized by green chemistry via Hibiscus Sabdariffa flower extract. *Journal of Alloys and Compounds*, 655, 314–320.
- Toyama, H., Higa, A., Yamazato, M., Maehama, T., Ohno, R., & Toguchi, M. (2006). Quantitative analysis of polarization phenomena in CdTe radiation detectors. *Japanese Journal of Applied Physics*, 45(11R), 8842.
- Travas-Sejdic, J., Peng, H., Cooney, R. P., Bowmaker, G. A., Cannell, M. B., & Soeller, C. (2006). Amplification of a conducting polymer-based DNA sensor signal by CdS NPs. *Current Applied Physics*, 6(3), 562–566.
- Usharani, K., Balu, A. R., Nagarethinam, V. S., & Suganya, M. (2015). Characteristic analysis on the physical properties of nanostructured Mg-doped CdO thin films—Doping concentration effect. *Progress in Natural Science: Materials International*, 25(3), 251–257.
- Wageh, S., Higazy, A. A., & Algrade, M. A. (2011). optical properties and activation energy of a novel system of CdTe NPs embedded in phosphate glass matrix. *Journal of Modern Physics*, 2(08), 913.
- Waghulade, R. B., Patil, P. P., & Pasricha, R. (2007). Synthesis and LPG sensing properties of nano-sized cadmium oxide. *Talanta*, 72(2), 594–599.
- Wang, G., Jin, L., Dong, Y., Niu, L., Liu, Y., Ren, F., et al. (2014). Multifunctional Fe₃O₄–CdTe@ SiO₂–carboxymethyl chitosan drug nanocarriers: Synergistic effect towards magnetic targeted drug delivery and cell imaging. *New Journal of Chemistry*, 38(2), 700–708.
- Wang, Y., Ramanathan, S., Fan, Q., Yun, F., Morkoc, H., & Bandyopadhyay, S. (2006). Electric field modulation of infrared absorption at room temperature in electrochemically self assembled QDs. *Journal of Nanoscience and Nanotechnology*, 6(7), 2077–2080.
- Wang, Y., Tang, Z., Tan, S., & Kotov, N. A. (2005). Biological assembly of nanocircuit prototypes from protein-modified CdTe NWs. *Nano Letters*, 5(2), 243–248.
- Wei, H., Zhou, J., Zhang, L., Wang, F., Wang, J., & Jin, C. (2015). The core/shell structure of CdSe/ZnS QDs characterized by X-ray absorption fine spectroscopy. *Journal of Nanomaterials*, 2015, 3.
- Willardson, R. K., & Beer, A. C. (1977). *Semiconductors and semimetals* (Vol. 12). Cambridge: Academic Press.
- Williams, J. V., Kotov, N. A., & Savage, P. E. (2009). A rapid hot-injection method for the improved hydrothermal synthesis of CdSe NPs. *Industrial and Engineering Chemistry Research*, 48(9), 4316–4321.

- Wong, I. Y., Bhatia, S. N., & Toner, M. (2013). Nanotechnology: Emerging tools for biology and medicine. *Genes & Development*, 27(22), 2397–2408.
- Wu, X. J., Zhu, F., Mu, C., Liang, Y., Xu, L., Chen, Q., et al. (2010). Electrochemical synthesis and applications of oriented and hierarchically quasi-1D semiconducting nanostructures. *Coordination Chemistry Reviews*, 254(9), 1135–1150.
- Xu, H., Mo, R., Cheng, C., Ai, G., Chen, Q., Yang, S., et al. (2014). ZnSe/CdS/CdSe triple-sensitized ZnO nanowire arrays for multi-bandgap photoelectrochemical hydrogen generation. *RSC Advances*, 4(88), 47429–47435.
- Yakuphanoglu, F. (2011). Synthesis and electro-optic properties of nanosized-boron doped cadmium oxide thin films for solar cell applications. *Solar Energy*, 85(11), 2704–2709.
- Yang, J., Gao, Y., Kim, J. W., He, Y., Song, R., Ahn, C. W., et al. (2010). Self-reorganization of CdTe NPs into two-dimensional Bi₂Te₃/CdTe nanosheets and their thermoelectrical properties. *Physical Chemistry Chemical Physics*, 12(38), 11900–11904.
- Yao, W. T., Yu, S. H., Liu, S. J., Chen, J. P., Liu, X. M., & Li, F. Q. (2006). Architectural control syntheses of CdS and CdSe nanoflowers, branched NWs, and nanotrees via a solvothermal approach in a mixed solution and their photocatalytic property. *The Journal of Physical Chemistry B*, 110(24), 11704–11710.
- Yildiz, I., McCaughan, B., Cruickshank, S. F., Callan, J. F., & Raymo, F. M. (2009). Biocompatible CdSe-ZnS core-shell QDs coated with hydrophilic polythiols. *Langmuir*, 25(12), 7090–7096.
- Yin, X. L., Li, L. L., Jiang, W. J., Zhang, Y., Zhang, X., Wan, L. J., et al. (2016). MoS₂/CdS nanosheets-on-nanorod heterostructure for highly efficient photocatalytic H₂ generation under visible light irradiation. *ACS Applied Materials & Interfaces*, 8(24), 15258–15266.
- Yu, H., Li, J., Loomis, R. A., Lin-Wang, W., & Buhro, W. E. (2003a). Two-versus three-dimensional quantum confinement in indium phosphide wires and dots. *Nature Materials*, 2(8), 517.
- Yu, W. W., Qu, L., Guo, W., & Peng, X. (2003b). Experimental determination of the extinction coefficient of CdTe, CdSe, and CdS NCs. *Chemistry of Materials*, 15(14), 2854–2860.
- Yu, Z., Tetard, L., Zhai, L., & Thomas, J. (2015). Supercapacitor electrode materials: nanostructures from 0 to 3 dimensions. *Energy & Environmental Science*, 8(3), 702–730.
- Zhang, J., Yang, Q., Cao, H., Ratcliffe, C. I., Kingston, D., Chen, Q. Y., et al. (2016). Bright gradient-alloyed CdSe_xS_{1-x} QDs exhibiting cyan-blue emission. *Chemistry of Materials*, 28(2), 618–625.
- Zhang, Y., Grady, N. K., Ayala-Orozco, C., & Halas, N. J. (2011). Three-dimensional nanostructures as highly efficient generators of second harmonic light. *Nano Letters*, 11(12), 5519–5523.
- Zhang, Y., Wang, L. W., & Mascarenhas, A. (2007). “Quantum coaxial cables” for solar energy harvesting. *Nano Letters*, 7(5), 1264–1269.
- Zhao, Y. S., Fu, H. B., Hu, F. Q., Peng, A. D., Yang, W. S., & Yao, J. N. (2008). Tunable emission from binary organic one-dimensional nanomaterials: An alternative approach to white-light emission. *Advanced Materials*, 20(1), 79–83.
- Zhong, Z., Qian, F., Wang, D., & Lieber, C. M. (2003). Synthesis of p-type gallium nitride NWs for electronic and photonic nanodevices. *Nano Letters*, 3(3), 343–346.
- Zhu, H., Jiang, R., Xiao, L., Chang, Y., Guan, Y., Li, X., et al. (2009). Photocatalytic decolorization and degradation of Congo Red on innovative crosslinked chitosan/nano-CdS composite catalyst under visible light irradiation. *Journal of Hazardous Materials*, 169(1), 933–940.
- Zhu, L., Li, C., Li, Y., Feng, C., Li, F., Zhang, D., et al. (2015). Visible-light photodetector with enhanced performance based on a ZnO@ CdS heterostructure. *Journal of Materials Chemistry C*, 3(10), 2231–2236.
- Zhu, Y., Mei, T., Wang, Y., & Qian, Y. (2011). Formation and morphology control of NPs via solution routes in an autoclave. *Journal of Materials Chemistry*, 21(31), 11457–11463.

- Zhu, Y., Mendelsberg, R. J., Zhu, J., Han, J., & Anders, A. (2013). Dopant-induced band filling and bandgap renormalization in CdO: In films. *Journal of Physics. D. Applied Physics*, *46*(19), 195102.
- Zyoud, A. H., Zaatar, N., Saadeddin, I., Ali, C., Park, D., Campet, G., et al. (2010). CdS-sensitized TiO₂ in phenazopyridine photo-degradation: Catalyst efficiency, stability and feasibility assessment. *Journal of Hazardous Materials*, *173*(1), 318–325.

Cadmium based II-VI Semiconducting Nanomaterials
Synthesis Routes and Strategies

Majid, A.; Bibi, M.

2018, XVI, 181 p. 45 illus., 29 illus. in color., Hardcover

ISBN: 978-3-319-68752-0